2008

# The electronic spectrum of TaO and its hyperfine structure

Kara J. Manke
T. R. Vervoort
Keith T. Kuwata, *Macalester College*
Thomas D Varberg, *Macalester College*

# Electronic spectrum of TaO and its hyperfine structure

Kara J. Manke,[a] Tyson R. Vervoort, Keith T. Kuwata, and Thomas D. Varberg[b]
*Department of Chemistry, Macalester College, 1600 Grand Ave., St. Paul, Minnesota 55105, USA*

(Received 4 December 2007; accepted 2 January 2008; published online 10 March 2008)

The $B\,^2\Phi_{5/2}-X_1\,^2\Delta_{3/2}(0,0)$ band at 778 nm and the $C\,^2\Delta_{3/2}-X_1\,^2\Delta_{3/2}(0,0)$ band at 737 nm of tantalum oxide (TaO) were recorded by laser excitation spectroscopy using a hollow cathode sputtering source to generate the molecules. The hyperfine structure arising from the $^{181}$Ta ($I=7/2$) nucleus was measured at sub-Doppler resolution using the technique of intermodulated fluorescence spectroscopy. The hyperfine structure was assigned and fitted in order to derive accurate values for the magnetic dipole and electric quadrupole interactions. The magnetic hyperfine constant for the ground electronic state was also calculated using the density functional theory as $h_{3/2}=625$ MHz, in good agreement with the experimental value of $647\pm10$ MHz. This result suggests that the $X\,^2\Delta$ ground state of TaO is well described by a pure $\delta\sigma^2$ electronic configuration, where the unpaired electron is located in a Ta $5d\delta$ orbital. © *2008 American Institute of Physics*. [DOI: 10.1063/1.2837470]

## I. INTRODUCTION

We began this study of the electronic spectrum of tantalum monoxide (TaO) following a search for spectra of tantalum monohydride (TaH) in the visible region. We have identified several bands in the visible spectrum of both TaH and TaD, which we will report separately.[1] Strong spectra of TaO were observed in these searches, which were undertaken using a low-resolution pulsed dye laser. When recorded with a continuous-wave ring laser, the spectra showed partially resolved hyperfine structure at Doppler-limited resolution. Since the hyperfine structure of TaO has never been reported in the literature, we proceeded to investigate it in order to shed light on the electronic character of the ground and excited states of TaO.

There have been a number of experimental studies undertaken on tantalum monoxide. One of the earliest was a study of its electronic spectrum in the gas phase by Premaswarup and Barrow.[2,3] Weltner and McLeod[4] recorded the electronic spectrum of TaO isolated in rare gas matrices, from the near infrared to the near ultraviolet. These authors identified transitions from the ground state to 17 different electronic states. This work motivated Cheetham and Barrow[5] to undertake a more extensive analysis of the gas-phase spectrum in emission, which included a rotational (and in some cases, vibrational) characterization of 19 different electronic states or substates. Most of the bands terminated in the $\Omega=3/2$ ground state, but they also observed emission to a low-lying $\Omega=5/2$ state with similar rotational and vibrational constants, located 3505 cm$^{-1}$ above the ground state. In light of the expected molecular orbital diagram for the molecule, this observation led them to postulate the ground state to be $\delta\sigma^2\,^2\Delta_r$.

The magnetic circular dichroism (MCD) spectrum of TaO trapped in a rare gas matrix has been measured by Brittain *et al.*,[6] who confirmed the $\Omega$ assignments of several of the upper states analyzed in Ref. 5. The phase of the MCD signal unambiguously provides the value of $\Delta\Omega$ for a transition, with $\Delta\Omega=0$ transitions being absent. The photoelectron spectrum of gaseous TaO has been recorded by Dyke *et al.*[7] Finally, the emission spectrum of the gaseous molecule has recently been reinvestigated by two groups. Ram and Bernath[8] measured several vibrational bands of two new electronic transitions near 500 nm. Al-Khalili *et al.*[9] recorded the emission spectrum from the near-infrared to the near-ultraviolet, reanalyzing several transitions that Cheetham and Barrow[5] had studied, as well as several that they had not. The TaO molecule has also been the subject of six computational studies, concerned with calculating the bond lengths, vibrational frequencies, and relative energies of the ground electronic state and the first excited quartet state $a\,^4\Sigma$.[10–15]

## II. EXPERIMENT

The $B\,^2\Phi_{5/2}-X_1\,^2\Delta_{3/2}(0,0)$ band at 778 nm and the $C\,^2\Delta_{3/2}-X_1\,^2\Delta_{3/2}(0,0)$ band at 737 nm of TaO were recorded by laser excitation spectroscopy using a hollow cathode sputtering source to generate the molecules. Argon with a trace of hydrogen was flowed through a small hole in a 12 mm diameter tantalum cathode, and a 30 mA dc electric discharge was struck and maintained. The addition of hydrogen stabilized the discharge, improving the signal-to-noise ratio. The resulting plasma was expanded downward through a 3 mm wide slit into a chamber maintained at approximately 1.0 Torr. The laser beam entered the vacuum chamber horizontally, crossing the molecular flow parallel to and 1 cm below the slit. Molecular fluorescence was collected by a 150 mm lens and passed through a (red-pass) colored glass filter that transmitted the excitation wavelength. This filter

[a]Current address: Department of Chemistry, Massachusetts Institute of Technology, Cambridge, MA 02139, USA.
[b]Electronic mail: varberg@macalester.edu.

 

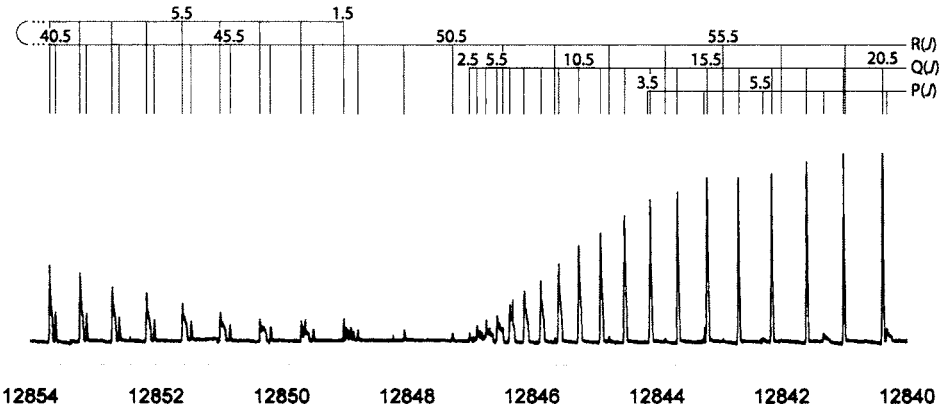


FIG. 1. Portion of the $B\,^2\Phi_{5/2}-X_1\,^2\Delta_{3/2}(0,0)$ band of TaO recorded at Doppler-limited resolution. The head of the $R$ branch forms at $R(24.5)$, near 12 857.3 $cm^{-1}$, which is 3.3 $cm^{-1}$ off to the left in this figure. The hyperfine broadening of the low-$J$ lines in each rotational branch is apparent.

blocked shorter-wavelength emission from the argon discharge, improving the signal-to-noise ratio. The fluorescence was then focused onto a side-on photomultiplier tube (Hamamatsu R928).

Our first spectra of TaO were observed using the output of a low-resolution ($\sim$0.1 $cm^{-1}$ bandwidth) pulsed dye laser, with fluorescence signals collected and integrated using a digital oscilloscope. Subsequently, high-resolution spectra were recorded using a single-mode Ti:sapphire ring laser (Coherent 899-29 pumped by a Coherent Verdi V-10 laser). The laser output was mechanically chopped, and the fluorescence signal was demodulated with a lock-in amplifier (Stanford SR510). The laser wavelength scanning and signal digitizing functions were carried out by the ring laser's dedicated computer. The linewidth of the laser radiation is less than 1 MHz, so that Doppler broadening was the major contributor to the observed spectral line widths of about 450 MHz.

Tantalum has only one significantly abundant isotope, namely, $^{181}$Ta (>99.9% abundance). The nuclear spin of $^{181}$Ta is $I=7/2$, with reasonably large magnetic ($2.37\mu_N$) and quadrupole (328 $fm^2$) moments.[16] At Doppler-limited resolution, the $^{181}$Ta hyperfine structure was partially resolved for only the first few lines in each rotational branch of both bands, with higher-$J$ lines showing unresolved broadening. In order to fully resolve this structure, we recorded each band at sub-Doppler resolution using intermodulated fluorescence spectroscopy.[17] Here we split the laser radiation into two beams with a 50/50 beamsplitter and chopped each beam at a different frequency. The beams were then counterpropagated through the vacuum chamber and crossed nearly collinearly in the center of the molecular flow. Each beam was about 125 mW in power before chopping and was focused down to 2 mm in diameter. The lock-in amplifier was referenced to the difference frequency of the two beams in order to record Lamb dips. The frequency scan rate was 25 MHz/s with a lock-in time constant of 300 ms. The ring laser's wavemeter was calibrated absolutely by recording optogalvanic spectra of atomic argon using a Nb metal hollow cathode lamp filled with argon.[18] The sub-Doppler lines had line widths of $\sim$40 MHz, presumably limited by pressure broadening. We estimate that the sub-Doppler features can be measured with an uncertainty of 0.001 $cm^{-1}$.

## III. RESULTS

### A. Assignment of the spectrum

Rotational assignments for the lines of the $B$-$X$ and $C$-$X$ (0,0) bands were made in a straightforward manner, using the upper and lower state rotational constants from the work of Cheetham and Barrow.[5] For the $B\,^2\Phi_{5/2}-X_1\,^2\Delta_{3/2}(0,0)$ band, single $R$, $Q$, and $P$ branches were observed, with the $Q$ branch being the strongest, consistent with the assignment of the band as a perpendicular ($\Delta\Omega=\pm1$) transition. A portion of this band near the origin is shown in Fig. 1. The first lines observed in the $R$ and $Q$ branches, $R(1.5)$ and $Q(2.5)$, unambiguously assign the transition as $\Omega=5/2-3/2$. The low-$J$ $P$ lines are very weak and could only be measured down to $P(4.5)$. In the limit of Hund's case (a) coupling, the transition selection rule $\Delta\Sigma=0$ then provides the symmetry assignment as $\Delta\Lambda=\Delta\Omega=+1$. Given the large spin-orbit splittings in TaO (3505 $cm^{-1}$ in the $X\,^2\Delta_r$ state[5]), the states are best described as intermediate between Hund's case (a) and (c) couplings. In this work, we maintain the case (a) labels used in previous studies of the molecule.

In the $C\,^2\Delta_{3/2}-X_1\,^2\Delta_{3/2}(0,0)$ band, Cheetham and Barrow[5] observed only $P$ and $R$ branches, and assigned a value of $\Omega'=3/2$ on that basis. With our lower temperature spectrum, we were able to observe a very weak $Q$ branch in this band and make sub-Doppler measurements of a few hyperfine components of the $Q(1.5)$, $Q(2.5)$, and $Q(3.5)$ lines. The first lines observed in this band are $R(1.5)$, $Q(1.5)$, and $P(2.5)$, confirming the $\Omega=3/2-3/2$ assignment. The $\Omega$ assignments for the $B$-$X$ and $C$-$X$ transitions are also consistent with those given in the MCD spectrum of Ref. 6.

The assignment of the hyperfine structure of the lines recorded at sub-Doppler resolution proceeded with little difficulty. For rotational transitions with $J''>7.5$, only the eight "main" $\Delta F=\Delta J$ hyperfine components were observed, and the $F$ quantum numbers could be assigned by their relative intensities. However, for the first few members of each rotational branch, we observed and measured weaker $\Delta F\neq\Delta J$ hyperfine "satellite" transitions. A good example of such transitions is shown in Fig. 2, which displays the sub-Doppler spectrum of the first $R$ line in the $B$-$X$ band. We were able to resolve all twelve allowed ($\Delta F=0,\pm1$) hyperfine components of this transition. The lower trace of Fig. 2 is a synthetic spectrum generated from the calculated transi-

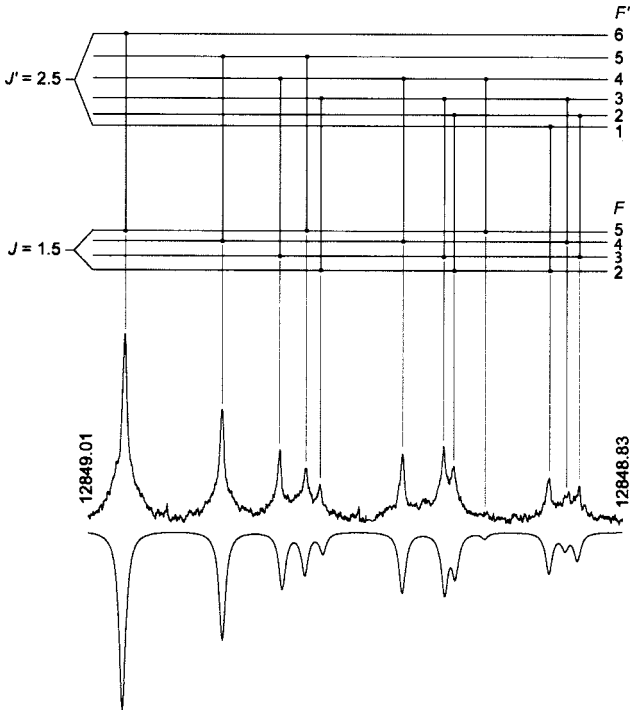


FIG. 2. Sub-Doppler spectrum of the first $R$ line $[R(1.5)]$ of the $B\,^2\Phi_{5/2}-X_1\,^2\Delta_{3/2}(0,0)$ band of TaO, recorded by intermodulated fluorescence spectroscopy. The relative energies of the hyperfine levels involved in this transition are shown above the spectrum, with tie lines identifying the individual components. There are 12 allowed hyperfine components, and all are resolved in this spectrum. The upper trace is the experimental spectrum; the lower trace is a simulated spectrum using calculated transition wavenumbers and intensities as described in the text.

tion wavenumbers of our least-squares fit, with 40 MHz wide (full width at half maximum) Lorentzian line shapes. The relative intensity $S$ of each component was calculated using the following formula:

$$S(J'IF \leftarrow JIF) \propto (2F+1)(2F'+1)\begin{Bmatrix} J' & F' & I \\ F & J & 1 \end{Bmatrix}^2.$$

The observation of satellite transitions is of benefit in the least-squares fitting of the bands, as they provide direct hyperfine combination differences for the two electronic states involved in the transition. For a few transitions, we determined the positions of satellite lines by the observation of center dips, especially where the satellite line was very weak or blended with another line. Center dips (or crossover resonances) are a consequence of the intermodulated fluorescence technique and are located exactly halfway in frequency between main and satellite lines that share a common energy level. If the frequency difference between the main and satellite lines is small compared to the Doppler width, then the center dip intensity is equal to the geometric mean of the intensities of the two transitions that produce it. Although the strongest branches in the two bands could be observed to about $J''=50.5$, we chose to measure and assign sub-Doppler spectra up to $J''=22.5$, as the higher-$J$ lines do not provide much additional useful information. No evidence of $\Omega$-doubling was seen in either band.

### B. The molecular Hamiltonian and least-squares fitting

Large spin-orbit splittings are observed in the electronic states of diatomic molecules containing a $5d$-transition metal atom. In the TaO ground $^2\Delta_r$ state, the observed spin-orbit splitting is 3505 $cm^{-1}$.[5,9] In such cases, the rotational levels are best described in a Hund's coupling case (c) basis, in which the observable quantum numbers are the total angular momentum $J$ and its projection along the internuclear axis $\Omega$.[19] We expressed our molecular Hamiltonian in this basis. The rotational and centrifugal distortion matrix elements were evaluated as

$$\langle J\Omega|\hat{H}|J\Omega\rangle = BJ(J+1) - DJ^2(J+1)^2. \quad (1)$$

In Hund's case (c) these matrix elements are more correctly written,[20]

$$\langle J\Omega|\hat{H}|J\Omega\rangle = B[J(J+1)-\Omega^2] - D[J^2(J+1)^2-\Omega^4], \quad (2)$$

but we have used Eq. (1) in order to be consistent with previous work on the molecule. The difference shows up only in the term energy of the upper state.

We then added matrix elements to represent the magnetic dipole and electric quadrupole interactions for the $^{181}$Ta nucleus. For the magnetic dipole interaction, the only determinable parameter in Hund's case (c) coupling is $h_\Omega$, which is a combination of the Frosch and Foley[21] hyperfine parameters: $h_\Omega = a\Lambda + (b+c)\Sigma = a\Lambda + (b_F + \frac{2}{3}c)\Sigma$. The true Fermi contact parameter $b_F$ is related to the parameter $b$ of Ref. 21 by the expression $b_F = b + \frac{1}{3}c$. The magnetic hyperfine structure has matrix elements obeying the selection rules $\Delta F=0$ and $\Delta J=0,\pm 1$. The electric quadrupole interaction $(e^2Qq_0)$ obeys the selection rules $\Delta F=0$ and $\Delta J=0,\pm 1,\pm 2$. We also included terms for the diagonal nuclear spin-rotation interaction $(c_I)$. These matrix elements were evaluated in a case $(c)$ basis as follows:[22]

$$\langle F,I,J,\Omega|\hat{H}|F,I,J,\Omega\rangle = \frac{h_\Omega R\Omega}{2J(J+1)} + e^2Qq_0W(3\Omega^2 - J(J+1)) + \frac{1}{2}c_IR, \quad (3)$$

$$\langle F,I,J,\Omega|\hat{H}|F,I,J-1,\Omega\rangle = -P(J)(h_\Omega + 3e^2Qq_0T\Omega)\left(\frac{4J^2-4\Omega^2}{4J^2-1}\right)^{1/2}, \quad (4)$$

$$\langle F,I,J,\Omega|\hat{H}|F,I,J-2,\Omega\rangle = 3e^2Qq_0Z\left(\frac{[J^2-\Omega^2][(J-1)^2-\Omega^2]}{[(2J-3)(2J-1)(2J+1)]}\right)^{1/2}, \quad (5)$$

where

$$R = F(F+1) - I(I+1) - J(J+1), \quad (6)$$

$$W = \frac{3R(R+1) - 4I(I+1)J(J+1)}{8I(2I-1)J(J+1)(2J-1)(2J+3)}, \quad (7)$$

TABLE I. Molecular constants (in $cm^{-1}$) for the $X\,^2\Delta_{3/2}$, $B\,^2\Phi_{5/2}$, and $C\,^2\Delta_{3/2}$ states of TaO. Values in parentheses represent one standard deviation in units of the last quoted digit.

| Constant | This work | Ref. 5 |
|---|---|---|
| | $X\,^2\Delta_{3/2}$ $(v=0)$ | |
| $B$ | 0.401 995 7 (40) | 0.401 930 (4)[a] |
| $10^7D$ | 2.882 (66) | 2.450 (2) |
| $h_{3/2}$ | 0.021 57 (17) | |
| $e^2Qq_0$ | −0.107 2 (16) | |
| | $B\,^2\Phi_{5/2}$ $(v=0)$ | |
| $T_0$ | 12 847.059 29 (11) | 12 852.02 (3) |
| $B$ | 0.386 852 0 (42) | 0.386 851 (10) |
| $10^7D$ | 3.056 (71) | 2.674 (8) |
| $h_{5/2}$ | 0.043 16 (13) | |
| $e^2Qq_0$ | −0.068 2 (18) | |
| | $C\,^2\Delta_{3/2}$ $(v=0)$ | |
| $T_0$ | 13 569.257 75 (13) | 13 569.27 (3) |
| $B$ | 0.387 544 2 (42) | 0.387 547 (9) |
| $10^7D$ | 3.013 (70) | 2.624 (8) |
| $h_{3/2}$ | 0.055 08 (21) | |
| $e^2Qq_0$ | −0.121 1 (18) | |
| $10^5c_1$ | 1.80 (28) | |
| rms error | 0.001 1 | |

[a]Value given is that of $B_0$ $(X\,^2\Delta_{3/2})$ from Ref. 5. Using the values of $B_e$ and $\alpha_e$ given in the abstract of Ref. 5 yields $B_0$=0.401 97 $cm^{-1}$, which is much closer to the value derived in the present work.

$$P(J)=\frac{[(F+I+J+1)(I+J-F)(F+J-I)(F+I-J+1)]^{1/2}}{4J}, \tag{8}$$

$$T=\frac{R+J+1}{4I(2I-1)(J-1)(J+1)}, \tag{9}$$

and

$$Z=\frac{P(J)P(J-1)}{I(2I-1)(2J-1)^{1/2}}. \tag{10}$$

The $B$-$X$ and $C$-$X$ (0,0) bands were fitted simultaneously using the Hamiltonian described above. The signal-to-noise ratio did not vary too widely across the rotational branches of the two bands, so we weighted each transition equally in the least-squares fit. A list of the observed and calculated transitions of the two bands has been deposited with the Electronic Physics Auxiliary Publication Service of the American Institute of Physics[23] and are also available from Varberg.

The results of the least-squares fitting are displayed in Table I. For the electronic term energies and rotational constants, these values are compared to those of Cheetham and Barrow.[5] For the two upper states, the rotational constants agree well with the previous work. Given the good agreement for the upper states, it is rather surprising that the ground state rotational constant does not agree with that of Ref. 5. However, as we indicate in a footnote to Table I, there may be a typographical error in the value of $B_0$ reported in Ref. 5. Our values for the rotational constants of all three states are larger than those reported in Ref. 9, but this may reflect the differences in the Hamiltonians used. Ram and Bernath[8] used a Hund's case (c) expression like ours in analyzing spectra of the $H$-$X$ and $K$-$X$ transitions, and their value for $B_0$ in the $X$ state is about four standard deviations from our value. The $C$ state term value reported here agrees well with that of Ref. 5, but the $B$ state term value inexplicably differs by nearly 5 $cm^{-1}$. However, our value does agree with that reported in Ref. 9, $T_0(B)$=12 847.0577 $cm^{-1}$.

### C. Hyperfine structure calculations

In order to understand the nature of the electronic states involved in our transitions, we undertook calculations of expectation values relevant to the magnetic hyperfine structure. The expectation value of $\langle r^{-3}\rangle_{5d}$ for the ground electronic state of TaO was deduced from the hyperfine coupling tensor calculated using the unrestricted density functional theory. The BHandHLYP hybrid functional[24] and the all-electron well-tempered basis set (WTBS) of Huzinaga and Miguel[25] were used both to optimize the geometry of TaO and compute the hyperfine constants. Hybrid functionals, which contain some Hartree-Fock (HF) exchange, provide more accurate descriptions of core-shell spin polarization than pure density functionals, and avoid the severe spin contamination of the unrestricted HF theory. These characteristics lead to the prediction of rather accurate hyperfine coupling constants, as reported by Remenyi *et al.*[26] and Saladino and Larsen.[27] The BHandHLYP functional we employed contains 50% HF exchange.[24] Following the approach of Astashkin *et al.*,[28] we fully decontracted the well-tempered basis set to maximize its flexibility in describing the core electron density. Tantalum was represented by a $(28s,21p,18d,12f)$ basis set, and oxygen was represented by a $(20s,13p)$ basis set.

The BHandHLYP/WTBS calculation predicts that $\langle r^{-3}\rangle_{5d}=4.571a_0^{-3}=3.084\times10^{31}$ $m^{-3}$. For a $5d$ electron, $|\langle\psi(r=0)\rangle|^2=0$, so the Fermi contact term due to the unpaired $5d$ electron by itself should be $b_F=0$. However, the $5d$ electron will induce some spin polarization of the electron density in the Ta core $s$ orbitals, leading to a nonzero Fermi contact term. The BHandHLYP/WTBS calculation predicts that $b_F$=102.7 MHz.

The contribution of a full unpaired $6s$ electron to the Fermi contact term $b_F$ was estimated by a calculation on the electronic state in which the singly occupied molecular orbital was Ta($6s$) in character. The BHandHLYP/WTBS method was again used to optimize the TaO geometry and to predict its hyperfine coupling constants. The calculation predicts that $b_F$=4189 MHz.

## IV. DISCUSSION

Magnetic hyperfine structure can be used to probe the electronic structure of a diatomic molecule, a consequence of the fact that the hyperfine parameters are proportional to certain expectation values of the molecule's unpaired electrons. In this way, the hyperfine structure can yield direct information about the molecular wavefunction. We begin such an analysis by considering the molecular orbital diagram for the

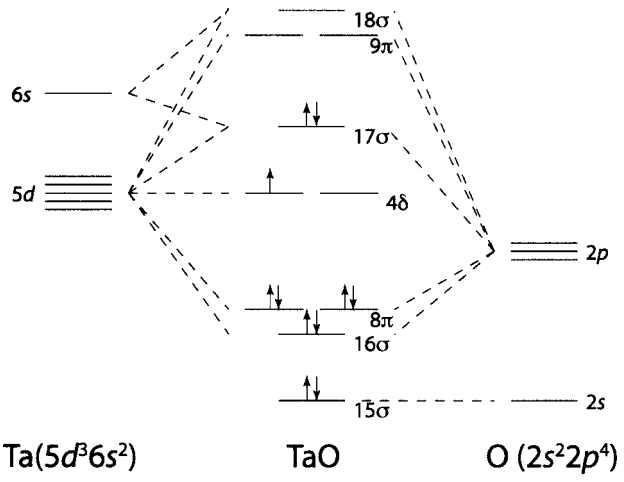


FIG. 3. The molecular orbital energy level diagram for TaO.

ground state of TaO, as shown in Fig. 3. All previous experimental studies[2–5,8,9] agree that the ground electronic state is $^2\Delta_r$ in the Hund's case (a) limit. The only reasonable molecular electronic configuration that gives rise to such a state is the one shown in Fig. 3: $(15\sigma)^2(16\sigma)^2(8\pi)^4(4\delta)^1(17\sigma)^2$, $^2\Delta_r$. Here, the $16\sigma$ bonding orbital is formed from overlap of the Ta $5d\sigma$ and O $2p\sigma$ orbitals; its antibonding counterpart is the $18\sigma$ orbital. The bonding $8\pi$ and antibonding $9\pi$ molecular orbitals are similarly formed from Ta $5d\pi$ and O $2p\pi$ atomic orbitals. The nonbonding $4\delta$ orbital containing the single unpaired electron is derived from Ta $5d\delta$. The $17\sigma$ orbital is also mostly nonbonding (Ta $5d\sigma$ and $6s$, with some O $2p\sigma$).

For a single unpaired electron, we can express the hyperfine parameters $a$, $b_F$, and $c$ as[29]

$$a = g\mu_B g_N \mu_N \left\langle \frac{1}{r^3} \right\rangle, \tag{11}$$

$$b_F = \frac{8\pi}{3} g\mu_B g_N \mu_N |\langle \psi(r=0) \rangle|^2, \tag{12}$$

$$c = \frac{3}{2} g\mu_B g_N \mu_N \left\langle \frac{3\cos^2\theta - 1}{r^3} \right\rangle. \tag{13}$$

Multiplying each of these equations on the right by the factor $10^{-6}\mu_0/4\pi h (=10^{-13}/h)$ expresses each parameter as a frequency in units of MHz. Since we have measured transitions out of just the lower $\Omega$-component of the doublet ground state, we can only obtain a value for an effective magnetic hyperfine parameter $h_\Omega$ that is a linear combination of these three: $h_\Omega = a\Lambda + (b_F + \frac{2}{3}c)\Sigma$. For $X_1\,^2\Delta_{3/2}$ ($\Lambda=+2$ and $\Sigma=-1/2$), this parameter is $h_{3/2} = 2a - \frac{1}{2}b_F - \frac{1}{3}c$. Using Eqs. (11)–(13), we can then predict the value of this parameter if we assume the unpaired electron is a pure Ta $5d\delta$ electron. The angular expectation value appearing in Eq. (13) has the value $\langle 3\cos^2\theta - 1\rangle_{d\delta} = -4/7$. Then, using the expectation value $\langle r^{-3}\rangle_{5d} = 4.571 a_0^{-3}$ from our density functional theory (DFT) calculation provides $a = 295.7$ MHz and $c = -253.5$ MHz. Together with the DFT value of $b_F = 102.7$ MHz produced by spin polarization, this leads to a predicted value of $h_{3/2} = 625$ MHz for the $X_1\,^2\Delta_{3/2}$ state. The fitted value of this parameter is $h_{3/2} = 647 \pm 10$ MHz ($2\sigma$ error limits). The agreement between the calculated and experimental values is very close, which suggests that the ground state does indeed arise mostly from the single configuration $\delta\sigma^2$, $^2\Delta_r$. We can further predict that the value of the magnetic hyperfine parameter in the $X_2\,^2\Delta_{5/2}$ level is $h_{5/2} = 2a + \frac{1}{2}b_F + \frac{1}{3}c = 558$ MHz.

The hyperfine structure of the upper electronic states in the two observed bands is more challenging to analyze. We postulate that both excited doublet states are derived from electronic configurations with three open subshells, namely, $(4\delta)^1(17\sigma)^1(9\pi)^1$ $B\,^2\Phi$ and $(4\delta)^1(17\sigma)^1(18\sigma)^1$ $C\,^2\Delta$, which means that their wavefunctions have to be written as linear combinations of Slater determinantal basis states.[20] Having measured the hyperfine structure in only one spin-orbit component of the upper states ($B\,^2\Phi_{5/2}$ and $C\,^2\Delta_{3/2}$), there is not enough information to perform a hyperfine analysis similar to that we have done for the ground state. We do note, however, that the fitted values of the hyperfine parameters $h_\Omega$ in the $B\,^2\Phi_{5/2}$ and $C\,^2\Delta_{3/2}$ states are 2.0 and 2.6 times larger, respectively, than the value in the ground state (see Table I). Since both proposed excited state configurations contain an unpaired electron in the $17\sigma$ (Ta $6s$) orbital, this is expected: our DFT result shows that an unpaired $6s$ electron would produce a Fermi contact interaction of 4189 MHz.

Finally, we note that of the group of six isovalent molecules VO,[30] NbO,[31] TaO, CrN,[32] MoN,[33] and WN,[34] all but TaO have a $^4\Sigma^-$ ground state derived from a $\delta^2\sigma$ configuration, with the $\delta\sigma^2\,^2\Delta$ state being a low-lying excited state. Only TaO has a $\delta\sigma^2\,^2\Delta$ ground state, which must reflect the fact that its $\delta$-$\sigma$ energy splitting is relatively small.

## V. CONCLUSION

Analyses of the $^{181}$Ta hyperfine structure of the $B\,^2\Phi_{5/2} - X_1\,^2\Delta_{3/2}(0,0)$ and $C\,^2\Delta_{3/2} - X_1\,^2\Delta_{3/2}(0,0)$ bands of TaO have determined values for the magnetic hyperfine and electric quadrupole parameters in the three electronic states for the first time. Using the density functional theory, a value for the $X_1\,^2\Delta_{3/2}$ magnetic hyperfine parameter $h_{3/2}$ has been calculated that is in excellent agreement with the experimentally determined value. This result demonstrates that the ground state is accurately described by a single electronic configuration, $\delta\sigma^2(^2\Delta_r)$.

## ACKNOWLEDGMENTS

Acknowledgment is made (by K.T.K.) to the Donors of the American Chemical Society Petroleum Research Fund for partial support of this research. This work has been supported by two grants (to T.D.V.) from the National Science Foundation (Grant Nos. CHE-0216172 and CHE-0518198). One of the authors (K.J.M.) thanks the Arnold Beckman Foundation for support in the form of a Beckman Scholarship. Two of the authors (K.T.K. and T.D.V.) both acknowledge the support from the Dreyfus Foundation for Henry Dreyfus Teacher-Scholar Awards. Calculations were performed at the National Center for Supercomputing Applications at the University of Illinois and the Midwest Undergraduate Computational Chemistry Consortium facility at

Hope College. The authors thank William Ames and David Ron, who recorded the initial low-resolution scans of TaO.

[1] T. D. Varberg, T. R. Vervoort, and K. J. Manke, presented at the American Chemical Society 233rd National Meeting, Chicago, IL, 2007 (unpublished).
[2] D. Premaswarup, Nature (London) **175**, 1003 (1955).
[3] D. Premaswarup and R. F. Barrow, Nature (London) **180**, 602 (1957).
[4] W. Weltner, Jr. and D. McLeod, Jr., J. Chem. Phys. **42**, 882 (1965).
[5] C. J. Cheetham and R. F. Barrow, Trans. Faraday Soc. **63**, 1835 (1967).
[6] R. Brittain, D. Powell, M. Kreglewski, and M. Vala, Chem. Phys. **54**, 71 (1980).
[7] J. M. Dyke, A. M. Ellis, M. Feher, A. Morris, A. J. Paul, and J. C. H. Stevens, J. Chem. Soc., Faraday Trans. 2 **83**, 1555 (1987).
[8] R. S. Ram and P. F. Bernath, J. Mol. Spectrosc. **191**, 125 (1998).
[9] A. Al-Khalili, U. Hällsten, and O. Launila, J. Mol. Spectrosc. **198**, 230 (1999).
[10] M. Dolg, H. Stoll, H. Preuss, and R. M. Pitzer, J. Phys. Chem. **97**, 5852 (1993).
[11] M. Zhou and L. Andrews, J. Phys. Chem. A **102**, 8251 (1998).
[12] M. Chen, X. Wang, L. Zhang, M. Yu, and Q. Qin, Chem. Phys. **242**, 81 (1999).
[13] F. Rakowitz, C. M. Marian, L. Seijo, and U. Wahlgren, J. Chem. Phys. **110**, 3678 (1999).
[14] F. Rakowitz, C. M. Marian, and L. Seijo, J. Chem. Phys. **111**, 10436 (1999).
[15] M. Zhou, J. Dong, L. Zhang, and Q. Qin, J. Am. Chem. Soc. **123**, 135 (2001).
[16] I. Mills, T. Cvitas, K. Homann, N. Kallay, and K. Kuchitsu, *Quantities, Units and Symbols in Physical Chemistry*, 2nd ed. (Blackwell, Oxford, 1993).
[17] M. S. Sorem and A. L. Schawlow, Opt. Commun. **5**, 148 (1972).
[18] S. J. Rixon and A. J. Merer (private communication).
[19] G. Herzberg, *Molecular Spectra and Molecular Structure I. Spectra of Diatomic Molecules*, 2nd ed. (Van Nostrand Reinhold, New York, 1950).
[20] H. Lefebvre-Brion and R. W. Field, *The Spectra and Dynamics of Diatomic Molecules* (Elsevier, Amsterdam, 2004).
[21] R. A. Frosch and H. M. Foley, Phys. Rev. **88**, 1337 (1952).
[22] A. G. Adam, Y. Azuma, J. A. Barry, A. J. Merer, U. Sassenberg, J. O. Schröder, G. Cheval, and J. L. Féménias, J. Chem. Phys. **100**, 6240 (1994).
[23] EPAPS, See EPAPS Document No. E-JCPSA6-128-010807 for 4 pages of observed and calculated transition wavenumbers. This document can be reached through a direct link in the online article's HTML reference section or via the EPAPS homepage (http://www.aip.org/pubservs/epaps.html).
[24] A. D. Becke, Phys. Rev. A **38**, 3098 (1988); A. D. Becke, J. Chem. Phys. **98**, 1372 (1993); C. Lee, W. Yang, and R. G. Parr, Phys. Rev. B **37**, 785 (1988).
[25] S. Huzinaga and B. Miguel, Chem. Phys. Lett. **175**, 289 (1990); S. Huzinaga and M. Klobukowski, *ibid.* **212**, 260 (1993).
[26] C. Remenyi, M. L. Muzarova, and M. Kaupp, J. Phys. Chem. B **109**, 4227 (2005); M. Munzarova and M. Kaupp, J. Phys. Chem. A **103**, 9966 (1999).
[27] A. C. Saladino and S. C. Larsen, J. Phys. Chem. A **107**, 1872 (2003).
[28] A. V. Astashkin, F. Neese, A. M. Raitsimring, J. J. A. Cooney, E. Bultman, and J. H. Enemark, J. Am. Chem. Soc. **127**, 16713 (2005); S. Kokatam, K. Ray, J. Pap, E. Bill, W. E. Geiger, R. J. LeSuer, P. H. Rieger, T. Weyhermuller, F. Neese, and K. Wieghardt, Inorg. Chem. **46**, 1100 (2007).
[29] T. D. Varberg, R. W. Field, and A. J. Merer, J. Chem. Phys. **95**, 1563 (1991).
[30] A. S.-C. Cheung, R. C. Hansen, and A. J. Merer, J. Mol. Spectrosc. **91**, 165 (1982).
[31] J. L. Femenias, G. Cheval, A. J. Merer, and U. Sassenberg, J. Mol. Spectrosc. **124**, 348 (1987).
[32] W. J. Balfour, C. X. W. Qian, and C. Zhou, J. Chem. Phys. **106**, 4383 (1997).
[33] R. C. Carlson, J. K. Bates, and T. M. Dunn, J. Mol. Spectrosc. **110**, 215 (1985).
[34] R. S. Ram and P. F. Bernath, J. Opt. Soc. Am. B **11**, 225 (1994); T. C. Steimle and W. L. Virgo, J. Chem. Phys. **121**, 12411 (2004).